THE SPECTRUM AND EXCITATION OF ELECTROMAGNETIC WAVES IN BISMUTH IN THE REGION OF HOLE CYCLOTRON RESONANCES

V. P. NABEREZHNIKH, D. E. ZHEREBCHEVSKIĬ and V. L. MEL'NIK

Donets Physico-technical Institute, Ukrainian Academy of Sciences

Submitted December 23, 1971

Zh. Eksp. Teor. Fiz. 63, 169—181 (July, 1972)

The surface impedance of bismuth plates in which magneto-plasma and cyclotron waves are excited is investigated theoretically and experimentally. The case when the direction of the magnetic field is perpendicular to the trigonal axis of the crystal along which the waves propagate ($\mathbf{H} \perp \mathbf{C}_3$, $\mathbf{C}_3 \parallel \mathbf{k}$) is considered in detail. It is shown that nonlocal conductivity effects result in the appearance of cyclotron waves (CW) near hole cyclotron resonances (CR). In contrast to previously observed CW the ones under consideration are elliptically polarized in a plane perpendicular to the stationary magnetic field (TM type waves) and for small values of kR (k is the wave number and R the cyclotron radius) the spectrum possesses normal dispersion and is compressed to the cyclotron resonance lines from the weak magnetic field side. Another consequence of the nonlocal effects is the appreciable change in the spectrum of a fast magnetosonic wave (MSW). As a result the MSW spectrum does not terminate at a hybrid resonance, as predicted by the local theory, but at the first hole resonance. The experimental investigation of the properties of the electromagnetic waves was carried out with 20—114 μ thick bismuth plates. By employing thin samples it was possible to observe surface impedance oscillations related to standing wave excitation not only in strong fields but also in the region of the first four CR harmonics for holes. The experimental and theoretical results are in both qualitative and quantitative agreement.

INTRODUCTION

IT is well known that high-frequency magnetoplasma waves (Alfven and fast magnetosonic waves) can propagate in compensated metals with equal numbers of electrons and holes ($n_1 = n_2$), in the presence of a constant magnetic field. By now these waves have been the subject of a considerable number of both theoretical[1-3] and experimental studies[3-8]. According to the theory, the spectrum and polarization of the magnetoplasma waves are linear ($\omega \sim kH$) in strong magnetic fields $\Omega \gg \omega$ (Ω is the cyclotron frequency and ω is the wave frequency). In weak magnetic fields, the spectrum may become nonlinear and the polarization elliptic. In particular, in a model in which the cyclotron masses of the different carriers differ strongly, as is the case, e.g., in bismuth, the spectrum of the Alfven wave ends at the frequency of the first cyclotron resonance (CR) if allowance is made for the time dispersion and for the difference between the Hall components of the conductivity tensor from zero, while the spectrum of a fast magnetosonic wave (MSW) propagating strictly in a transverse direction ends at the hybrid-resonance frequency $\Omega = \sqrt{\Omega_1\Omega_2}$[2]. This picture of the spectrum was obtained without allowance for the spatial dispersion. At the same time, in a magnetic field parallel to the surface of the metal, nonlocal effects and the conductivity of the metal should play an appreciable role near the resonance frequencies. One must therefore assume that the spatial dispersion can considerably alter the spectrum of the MSW at $\mathbf{k} \perp \mathbf{H}$ in the region of the cyclotron resonances. The experimental investigations performed to date were devoted mainly to the properties of magnetoplasma waves in the strong-field limit. Although in weak fields deviations from linearity were observed and were correctly interpreted as being due to the presence of spatial and temporal dispersion[7], no detailed study of the spectrum in the region of the cyclotron resonance was carried out. Another even more significant result, due to the spatial dispersion near the resonant frequencies, is the existence of cyclotron waves (CW). Theoretical investigations of CW[9,10] have shown that in metals with spherical Fermi surface in a magnetic field parallel to the surface of the metal there can propagate both short CW ($kR \gg 1$) and long ones ($kR \ll 1$).

The short-wave part of the spectrum has three branches and determines the propagation of linearly polarized waves. The spectra of the ordinary wave ($\mathbf{E} \parallel \mathbf{H}$, $\mathbf{E} \parallel \mathbf{k}$) and of extraordinary wave ($\mathbf{E} \perp \mathbf{H}$, $\mathbf{E} \perp \mathbf{k}$) have normal dispersion (positive phase velocity) and lie near the CR lines on the side of the strong magnetic fields. The third branch, pertaining to the longitudinal wave ($\mathbf{E} \parallel \mathbf{k}$), has anomalous dispersion and tends towards the CR lines from the weak-magnetic-field side.

In the long-wave part of the spectrum, only the ordinary wave has linear polarization, while the other two are elliptically polarized in a plane perpendicular to the magnetic field. All three long-wave branches have anomalous dispersion and lie near the CR on the side of the strong magnetic field. A similar picture was obtained for the ordinary CW in bismuth near the hole CR for those magnetic-field directions at which the cyclotron masses of the hole greatly exceed the electron masses[11].

The most experimental studies were made on the long-wave ordinary CW, which were observed in alkali metals[10] and in bismuth near the electron CR[12].

Good qualitative, and sometimes also quantitative agreement with the conclusions of the theory was obtained.

An entirely different situation, as shown in the present paper, arises in bismuth for CW with elliptic polarization (type TM wave).

Since an MSW with a polarization linear in strong fields but elliptic in weak fields can propagate in the CR region, an interaction between the MSW and the CW sets in. This leads to a strong change in the spectra of both the MSW and the CW. In particular, the MSW can end already at the frequency of the first full CR, and one of the CW branches has a normal dispersion and comes close to the CR lines on the weak-field side.

This singularity of the propagation of MSW in the region of hole CR was noted in [13-15]. However, the simplifications assumed in the description of the electronic spectrum of bismuth and of the dispersion equation did not permit the authors of these papers to obtain the correct picture of the spectrum in the resonance region.

The purpose of the present paper is to report a detailed theoretical and experimental study of the MSW and CW spectra near hole cyclotron resonances in bismuth and the conditions for the excitation of these waves in a plate [1]. We chose here the most interesting case ($\mathbf{k} \parallel C_3$; $\mathbf{H} \parallel C_1$), when the spatial dispersion exerts a particularly strong influence.

THEORY

We consider the case when a bismuth sample is placed in a constant magnetic field **H** parallel to the surface of the metal, and an electromagnetic wave of frequency ω is incident on its surface. The electromagnetic field in the metal is described by Maxwell's equations, which can be written, after eliminating the alternating magnetic field and changing over to Fourier representations, in the form

$$k^2\mathbf{E} - \mathbf{k}(\mathbf{kE}) = 4\pi i\omega c^{-2}\hat{\sigma}\mathbf{E} + \frac{\omega^2}{c^2}\varepsilon_0\mathbf{E}, \tag{1}$$

where **k** is the wave vector, **E** is the Fourier representation of the intensity of the high-frequency electric field, and $\hat{\sigma}$ is the Fourier representation of the conductivity tensor. The dispersion equation of the electromagnetic wave is obtained from the compatibility conditions of the system of homogeneous equations (1) by setting its determinant equal to zero. The last term in (1), which describes the displacement current, can be neglected in deriving the dispersion equation at $\omega \ll \omega_0$ (ω_0 is the plasma frequency of the metal). To solve the dispersion equation it is necessary to know the explicit dependence of the conductivity tensor on the wave vector and on the frequency of the electromagnetic field; this dependence is obtained by solving the kinetic equation for the carrier distribution function.

In a coordinate system in which the z axis is directed along **H** and the y axis coincides with the normal to the surface, the conductivity tensor $\sigma_{jk}(\omega, k)$, a general expression for which was obtained by Azbel' and Kaner for an arbitrary carrier dispersion [16], can be reduced to the form

$$\sigma_{jk} = \frac{4\pi e^2}{(2\pi\hbar)^3}\sum_{n=-\infty}^{\infty}\int_{-p_{zmax}}^{p_{zmax}} dp_z \frac{m a_{nj} a_{nk}^*}{\nu - i(\omega - n\Omega)}, \tag{2}$$

where

$$a_{nj} = \frac{1}{2\pi}\int_0^{2\pi} d\tau v_j(\tau)\exp\left(\frac{ikp_x}{m\Omega} - in\tau\right). \tag{3}$$

Here e is the electron charge, ν is the carrier collision frequency, p_x and p_z are the components of the momentum vector, v_j are the components of the velocity vector on the Fermi surface, and τ is the phase shift of the motion in a magnetic field. The first sum denotes summation over all types of carrier.

The Fermi surface of bismuth consists of three strongly elongated electronic ellipsoids, which are turned through 120° relative to each other around the trigonal axis of the crystal, and one hole ellipsoid. The energy of the hole ellipsoid is described by the equation

$$\varepsilon_h(p) = \frac{p_1^2}{2M_1} + \frac{p_2^2}{2M_1} + \frac{p_3^2}{2M_3}, \tag{4}$$

where p_1, p_2 and p_3 are the components of the momentum vector **p** along the bisector, binary, and trigonal axes, respectively, and the masses, according to [17], are $N_1 = 0.063m_0$ and $M_3 = 0.65m_0$, where m_0 is the free-electron mass. The energy of one of the electronic ellipsoids can be represented in the form

$$\varepsilon_e(p) = \frac{1}{2m_0}(\alpha_1 p_1^2 + \alpha_2 p_2^2 + \alpha_3 p_3^2 + 2\alpha_4 p_2 p_3), \tag{5}$$

and the expressions for the two other electronic ellipsoids can be obtained by rotating the first through 120° about the trigonal axis. According to [18], $\alpha_1 = 1.81$, $\alpha_2 = 167$, $\alpha_3 = 89.7$, $\alpha_4 = 7.8$.

If the magnetic-field vector lies in a plane perpendicular to the trigonal axis, and the wave vector is directed along this axis, then we have for the hole ellipsoid in the chosen coordinate system

$$\begin{gathered} p_x = \sqrt{2M_1(\varepsilon_\text{д} - p_z^2/2M_1)}\sin\tau, \\ p_y = \sqrt{2M_3(\varepsilon_\text{д} - p_z^2/2M_1)}\cos\tau, \\ v_x = p_x/M_1, \quad v_y = p_y/M_3, \quad M = \sqrt{M_1M_3}, \end{gathered} \tag{6}$$

where M is the cyclotron mass of the holes.

Substituting (6) in (2) and (3), we obtain for the transverse components of the hole conductivity

$$\sigma_{xx}^h = \frac{3Ne^2}{2M_1}\sum_n \frac{1}{\nu - i(\omega - n\Omega)}\int_0^\pi d\theta \sin^3\theta J_n'^2(kR\sin\theta),$$

$$\sigma_{yy}^h = \frac{3Ne^2}{2M_3}\frac{1}{(kR)^2}\sum_n \frac{n^2}{\nu - i(\omega - n\Omega)}\int_0^\pi d\theta \sin\theta J_n^2(kR\sin\theta),$$

$$\sigma_{xy}^h = -\sigma_{yx}^h = -\frac{3Ne^2}{2M}\frac{i}{kR}\sum_n \frac{n}{\nu - i(\omega - n\Omega)} \times \int_0^\pi d\theta \sin^2\theta J_n(kR\sin\theta)J_n'(kR\sin\theta),$$

$$\sigma_{xz} = \sigma_{zx} = \sigma_{yz} = \sigma_{zy} = 0, \tag{7}$$

where N is the hole concentration and R is the effective cyclotron radius of the holes of the central cross section ($p_z = 0$).

We now consider the conductivity due to the electron ellipsoids.

We denote the angle between the direction of the magnetic field and the major axis of the electron ellipsoid by φ. At $\varphi = 0$, the cyclotron mass of the electrons $m = m_0/\sqrt{\alpha_2'\alpha_3'}$ (where α_2' and α_3' are the principal values

[1] Preliminary results were published earlier [13].

of the reciprocal-mass tensor) is much less than the cyclotron mass, and the effective radius of the electrons ($\mathbf{k} \perp \mathbf{H}$) is smaller than the radius of the holes. At nonzero φ, neglecting terms of order $\alpha_4^2/\alpha_2\alpha_3$ in comparison with unity, we readily obtain

$$\begin{aligned} m &= [\alpha_3(\alpha_2\cos^2\varphi_1 + \alpha_1\sin^2\varphi_1)]^{-1/2} m_0, \\ m_1 &= [\alpha_2\cos^2\varphi_1 + \alpha_1\sin^2\varphi_1]^{-1} m_0, \\ m_3 &= m_0/\alpha_3, \end{aligned} \tag{8}$$

where φ_1 is the angle between the major axis of the ellipsoid and the direction of the magnetic field in the plane perpendicular to the trigonal axis. The conductivity of the electron ellipsoid is also described by formulas (7) with the substitutions $N \to N/3$, $M_1 \to m_1$, $M \to m$, $M_3 \to m_3$ and with the Hall components of the conductivity taken with opposite sign. The cyclotron mass of the electrons at all angles not too close to $\pi/2$ ($\pi/2 - \varphi \gg \alpha_1/\alpha_2$), remains much smaller than the cyclotron mass of the holes, and at $kR < 1$ the electrons "feel" the spatial dispersion much less than the holes.

The spectrum of the electromagnetic waves polarized in a plane perpendicular to the magnetic field is determined, according to (1), by the equation

$$\frac{k^2c^2}{4\pi\omega i}\sigma_{yy} - \sigma_{xx}\sigma_{yy} + \sigma_{xy}\sigma_{yx} = 0. \tag{9}$$

Here σ_{jk} is the summary conductivity of the electron and hole ellipsoids. In the general case, it is difficult to obtain an analytic solution of (9), in view of the complexity of the expressions, and we shall therefore consider first, by way of example, the solution of this equation near the first two hole CR and the region of long wavelengths ($kR \ll 1$), where the expressions for the elements of the conductivity tensor can be replaced by their asymptotic expansion. At $\mathbf{H} \parallel \mathbf{C}_1$, the elements of the conductivity tensor have the following asymptotic forms:

$$\begin{aligned} \sigma_{xx} &= \frac{iNe^2}{M_1}\left[\frac{\omega}{\omega^2-\Omega^2}\left(1 - \frac{(kR)^2}{5} + \frac{(kR)^4}{56}\right)\right. \\ &\quad \left. + \frac{1}{10}\frac{(kR)^2}{\omega - 2\Omega}\left(1 - \frac{(kR)^2}{7} + \frac{(kR)^4}{108}\right)\right], \\ \sigma_{yy} &= \frac{iNe^2}{M_3}\left[\frac{\omega}{\omega^2-\Omega^2}\left(1 - \frac{3(kR)^2}{5} + \frac{37(kR)^4}{280}\right) - \frac{3m_0\omega}{\alpha_1 M_1\Omega^2}\right. \\ &\quad \left. + \frac{1}{10}\frac{(kR)^2}{\omega - 2\Omega}\left(1 - \frac{2(kR)^2}{7} + \frac{25(kR)^4}{756}\right)\right], \\ \sigma_{yx} &= \frac{Ne^2}{M}\left[\frac{\omega}{\omega^2-\Omega^2}\left(1 - \frac{2(kR)^2}{5} + \frac{3(kR)^4}{56}\right) + \frac{1}{\Omega} + \frac{1}{10}\right. \\ &\quad \left. \times\frac{(kR)^2}{\omega - 2\Omega}\left(1 - \frac{3(kR)^2}{14} + \frac{(kR)^4}{54}\right)\right]. \end{aligned} \tag{10}$$

Since the cyclotron mass of the electrons is much less than the cyclotron mass of the holes, the strong-magnetic-field condition ($\omega \ll \Omega_e$) is satisfied for the electrons near the first hole CR.

The solution of the dispersion equation takes in this case, near the frequencies of the first hole CR, the form

$$\frac{k^2c^2}{\omega_0^2}\left(1 - \frac{3m_0}{\alpha_1 M_1}\frac{\omega^2-\Omega^2}{\Omega^2}\right) - \frac{\omega^2}{\Omega^2} = 0{,}006\frac{(kR)^4}{\omega/\Omega - 1}, \tag{11}$$

and near the frequencies of the second hole resonance

$$\frac{k^2c^2}{\omega_0^2}\left(\frac{\omega^2}{\omega^2-\Omega^2} - \frac{3m_0}{\alpha_1 M_1}\frac{\omega^2}{\Omega^2}\right) - \frac{\omega^4}{\Omega^2(\omega^2-\Omega^2)}$$

$$= \frac{\omega(kR)^2}{10(\omega-2\Omega)}\left[\frac{2\omega^2}{(\omega+\Omega)\Omega} - \frac{k^2c^2}{\omega_0^2}\right] - \frac{1{,}9\cdot 10^{-6}\omega^2(kR)^8}{(\omega-2\Omega)^2} \tag{12}$$

where $\omega_0 = \sqrt{4\pi Ne^2/M_1}$ is the plasma frequency of the holes.

The left-hand sides of (11) and (12) describe the MSW spectrum, which in the absence of spatial dispersion ($kR \to 0$) terminates at the hybrid resonance frequency ($\omega^2/\Omega^2 = 1 + \alpha_1 M_1/3m_0$). When the spatial dispersion is taken into account, the MSW no longer crosses the lines of the first CR, and it goes over into a DW near this point with increasing k. The long-wave part of the CW spectrum has a normal dispersion near the fundamental harmonic of the hole resonance, and lies on the weak-field side. With increasing k, its spectrum moves sharply away from the resonance line and has the same character as the MSW spectrum in the absence of spatial dispersion; subsequently, however, as follows from (12) its spectrum, without reaching the second harmonic of the resonance, bends towards larger k. Near the second hole resonance (Eq. (12)) there are two branches of the CW spectrum, one of which has an anomalous dispersion and comes close to the resonance line on the side of the strong magnetic field, while the other behaves in analogy to the wave near the first resonance.

In the case of strong spatial dispersion, the asymptotic product of the Hall elements of the conductivity tensor is smaller by a factor kR than the product of the diagonal elements. The CW spectrum in bismuth at large kR is analogous to the spectrum in uncompensated metals; the latter was investigated by Kaner and Skobov[9]. The spectrum of electromagnetic waves at arbitrary kR was calculated with an electronic computer. We took into account the spatial dispersion of both the hole and the electrons of all three ellipsoids at the first nine harmonics of the cyclotron resonance. The expressions for the components of the conductivity tensor were expanded in powers of kR up to terms of order $(kR)^{40}$. The remaining terms (with larger n and of higher order in kR) do not exceed 10^{-10} at $kR < 5$ (a decrease in accuracy would not simplify the computation program). The error in the calculation of the spectrum does not exceed 0.01% in terms of ω/Ω.

The calculated MSW spectrum and one of the CW branches near the first free hole resonances at $kR \leq 4$ are shown in Fig. 1. The second CW branch lies very close to the cyclotron-resonance line and is not shown in the figure.

We consider now the excitation of electromagnetic waves in a metal plate of thickness d and with infinite dimensions in the other two directions. If there is no electric field on the surface of the plate, then the plate acts as a resonator and the wave vector k assumes discrete values. The eigensolutions of Maxwell's equations can be both symmetrical and antisymmetrical[19]

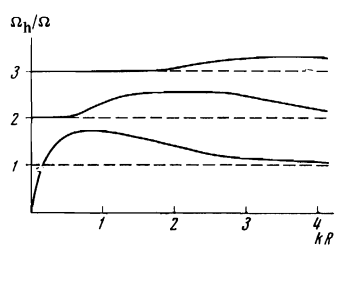

FIG. 1. Calculated spectrum of electromagnetic waves in bismuth in the region of the first three (1–3) harmonics of the hole cyclotron resonance, $\mathbf{k} \parallel c_3$, $\mathbf{H} \parallel c_1$.

$$E^{(s,a)}(y) = E^{(s,a)}(0)\cos k_l^{(s)} y, \quad k_l^{(s)} = 2\pi d^{-1}(l + {}^1/_2),$$
$$E^{(a)}(y) = \frac{[\mathbf{kH}^{(a)}]}{k}\frac{i\omega}{ck_l^{(a)}}\sin k_l^{(a)} y, \quad k_l^{(a)} = \frac{\pi l}{d}, \qquad (13)^*$$
$$-d/2 < y < d/2.$$

If an electromagnetic wave is incident on one side of the plate and only x- and z-components of the electric field are excited, then the fields $E^{(s)}$ and $E^{(a)}$ will exist in the place to equal degrees and the resonance will set in when half the wavelength is an exact multiple of the plate thickness. If the excited wave has also a y-component of the field, then, besides taking into account the ordinary boundary conditions ($E_x(d/2) = E_x(-d/2) = E_y(d/2) = E_y(-d/2)$), it is important to take into account the conditions of quasineutrality of the metal and of the charge conservation

$$\int_{V_{pl}} \rho\, dV = 0, \quad \partial\rho/\partial t = -\,div\,\mathbf{j}, \qquad (14)$$

which were previously satisfied automatically. Here ρ is the charge density, j is the conduction current, and V_{pl} is the volume of the plate.

Recognizing that all the quantities vary harmonically in time and the conductivity current, directed along **k**, is equal to displacement current $\omega^2 c^{-2} E_y$, as follows from (1), we get from (14)

$$\int_{-d/2}^{d/2} \frac{dE_y}{dy}\, dy = 0. \qquad (15)$$

In other words, the longitudinal electric field should satisfy the condition $E(-d/2) = E(d/2)$ and its distribution over the plate should be antisymmetrical. This means that the second of the two solutions in (13) will be realized, and the resonance will set in at a plate thickness which is a multiple of the wavelength or $k_l = 2\pi l/d$.

In the considered case of wave propagation in bismuth, the longitudinal component of the electric field is equal to $E_y = i(\sigma_{xy}/\sigma_{yy})E_x$ and varies with the magnetic field. E_y is small in strong fields, so that the wave is practically linearly polarized along x, while on the sections of the spectrum with anomalous dispersion ($kR \gg 1$) is almost purely longitudinal. Such a dependence of the degree of ellipticity of the polarization on the magnetic field can cause the excitation of both symmetrical and antisymmetrical fields in the region of strong fields. With decreasing magnetic field and increasing E_y, the symmetrical fields will attenuate more strongly, so that starting with a certain magnetic field, the plate will resonate only for antisymmetrical field, and its impedance will be described by the formula

$$Z = \frac{4\pi i\omega}{kc^2}\,\mathrm{tg}\,\frac{kd}{2}, \qquad (16)$$

where the relation $k = k'(\omega) + ik''(\omega)$ is determined from the dispersion equation (9). Since the mechanism whereby the electromagnetic waves are damped at $\mathbf{k} \perp \mathbf{H}$ is purely collisional, we can write in the first approximation in ν/ω ($\nu/\omega \ll 1$ is the necessary condition for the existence of weakly-damped waves)

$$k(\omega, \omega + i\nu) \approx k(\omega) + i\nu\frac{dk}{d(i\nu)}. \qquad (17)$$

*$[\mathbf{kH}] \equiv \mathbf{k} \times \mathbf{H}$.

In that part of the spectrum where the greatest importance is played by the frequency dependence of the conductivity tensor ($k^2c^2/4\pi\omega \ll \sigma$) we have $dk/d(i\nu) \approx dk/d\omega$, and in the linear part of the magnetostatic-wave spectrum we have $dk/d(i\nu) = {}^1/_2\, dk/d\omega$. It follows therefore that the relative amplitude of the spikes of surface impedance is determined by the inclination of the spectral lines of the electromagnetic waves. Figure 2 shows the graphically constructed dependence of the maximum value of the surface-impedance spikes on the reciprocal magnetic field when standing electromagnetic waves whose spectrum is shown in Fig. 1 are excited in a plate 64 μ thick ($\nu/\omega \approx 10^{-2}$).

EXPERIMENTS

The experimental study of the electromagnetic-wave spectrum in bismuth of strong spatial dispersion was carried out a frequency f = 36 GHz in the temperature interval 1.5—4.2° K. The samples where plane-parallel plates of bismuth 0.02, 0.064, 0.09, and 0.146 mm thick, in the shape of disks of 8 mm diameter. The flat surfaces of all the samples coincided with the trigonal plane of the crystal. The technology of sample preparation consisted of the following. A single crystal rod of 8 mm diameter with trigonal axis coinciding with the rod axis was grown from the initial ingot of bismuth with a room-to-helium-temperature resistance ratio ~ 150. After cleaving the rod in liquid nitrogen into several parts, polished brass disks were fastened to the mirror-finished surfaces with GKZh-94 oil. Repeated cooling and cleaving has made it possible to obtain thin plates frozen to the brass disks.

After heating and drying, the bismuth samples together with the disks were placed in a cartridge in a special rectangular resonator, the construction of which is described in[20]. A feature of this resonator is that the sample, while serving as the bottom of the resonator, has no mechanical contact with it. The sample can be rotated relative to the polarization of the high-frequency current; this polarization is linear in the resonator. The fastening of the sample to the bottom of the cartridge with oil did not greatly influence the magnitude of the effect.

To be able to prepare the samples successfully by this method, it is necessary that the bismuth rod be a high-grade single crystal, for only when a perfect single crystal is broken up by cleavage are the cleaved surfaces ideal planes.

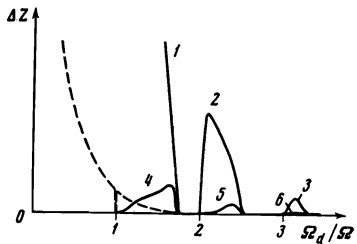

FIG. 2. Amplitude of surface-impedance oscillations when standing electromagnetic waves are excited in a bismuth plate 0.064 mm thick at $\nu/\omega = 10^{-2}$ in relative units. The numbers 1, 2, and 3 denote the envelopes of the impedence oscillations upon excitation of parts of the wave spectrum with normal dispersion, and the numbers 4, 5, and 6 pertain to anomalous dispersion. The dashed line shows (in a scale 1:100) amplitude of the oscillations of the surface impedance upon excitation of a magnetosonic wave.

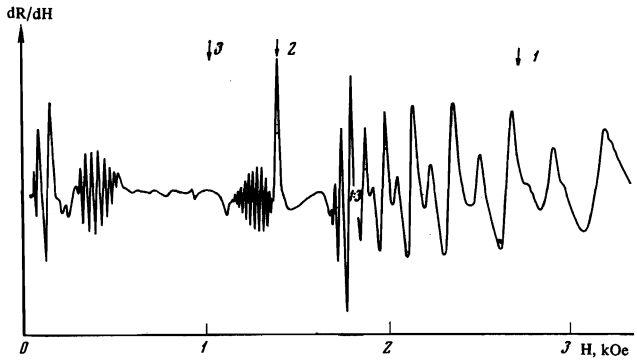

FIG. 3. Experimental plots of the derivative of the surface impedence against the magnetic field upon excitation of standing electromagnetic waves in a bismuth plate 0.064 mm thick at 1.5°K, $\mathbf{H} \parallel C_1$ and $\mathbf{j} \parallel C_2$. The numbers 1, 2, and 3 denote the first hole cyclotron resonances.

The sample thickness was measured with a vertical optimeter accurate to 2 μ. Since the contact method spoils the samples, the thicknesses were measured after the experiments. During the time of the experiment, the magnetic field was in the plane of the sample, and the direction of the high-frequency current was perpendicular to **H**. The magnetic field was made parallel to the surface of the sample by setting the CR lines to maximum. The magnetic field intensity was measured by a Hall pickup calibrated by nuclear resonance.

The existence of standing waves in the bismuth sample was revealed by oscillations of the derivative of the surface resistance with respect to the magnetic field. A typical plot of dR/dH against H is shown in Fig. 3. In strong fields one observes intense oscillations, which should be attributed, according to the universally accepted concepts, to excitation of standing waves due to the MSW. However, as will be shown in the discussion, some of them are due to MSW and some to CW. The shown dependence of their amplitude on a magnetic field is not the true one, since large changes of the plate impedance lead to a strong change in the coupling of the resonator with the waveguide line, and this could cause considerable detuning when a bridge circuit and a reflecting resonator are used. The amplitude of the oscillations can be estimated from the fact that the first hole CR line is hardly visible against their background.

Near the hole CR lines, starting with the second, there are observed oscillations due to the CW. Their amplitude depends very strongly on the temperature. As seen from Fig. 4, which shows the experimental plots of

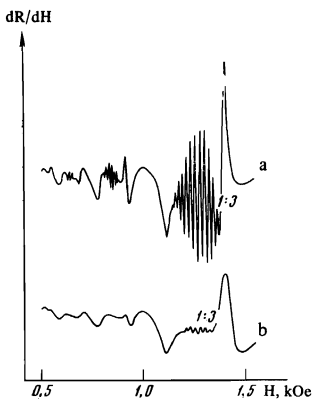

FIG. 4. Plot of oscillations of dR/dH upon excitation of cyclotron waves in a bismuth plate 0.064 mm thick at different temperatures: a–1.5°K, b–3.5°K.

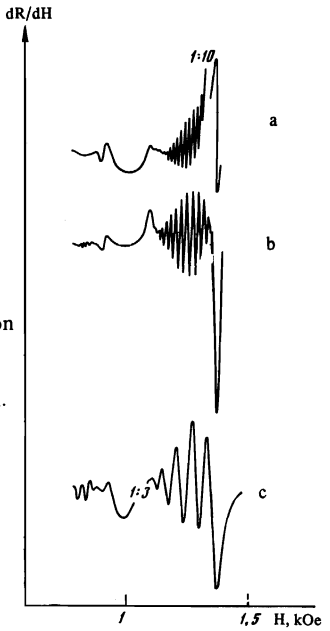

FIG. 5. Plot of oscillations of dR/dH upon excitation of cyclotron waves near the second hole cyclotron resonance in bismuth plates with different thicknesses at 1.5°K. $\mathbf{H} \parallel C_1$, $\mathbf{j} \parallel C_2$. a–0.09 mm, b–0.064 mm, c–0.02 mm.

the oscillations near the second, third, and fourth CR lines at different temperatures, an increase of the temperature from 1.5 to 3.5° K causes oscillations of noticeable amplitude to remain only near the second line. If the CR amplitude is decreased by a factor 1.5, then the oscillation amplitude is decreased by a factor of 18. Figure 5 shows the amplitude of the oscillations near the second CR with changing sample thickness at T = 1.5°K. We see that the ratio of the amplitudes of the CR lines and oscillations, equal to 1.5 at a thickness 0.02 mm, increases to ~ 25 at a thickness 0.09 mm. When the magnetic field is rotated in the plane of the sample, the amplitude and the period of the oscillations change. They are most intense when $\mathbf{H} \parallel C_1$ and $\mathbf{H} \perp \mathbf{j}$.

In weaker fields near the first electron CR line there are also observed oscillations at $\mathbf{H} \perp \mathbf{j}$, due apparently to a CW of another type. The properties of these waves were not investigated in the present study and will be dealt with in a separate article.

DISCUSSION OF RESULTS

Summarizing the conclusions of the theory, we can state that in bismuth in strong magnetic fields, and also in the region of hole CR, there can propagate an entire series of transverse-magnetic waves of the TM type, whose electric field vector lies in a plane perpendicular to H. The ellipticity of their polarization depends significantly on the magnetic-field region, so that the waves can go over from transverse TEM to purely longitudinal ones.

These waves can be arbitrarily broken up into three types: magnetosonic wave, whose spectra begins in very strong fields and terminates at the frequency of the first hole CR, long-wave cyclotron waves with normal dispersion, and short-wave cyclotron waves with anomalous dispersion.

In turn, the spectrum of some CW lies in the cyclotron-frequency region on the side of the weak magnetic field and deviates strongly from them, and the spectrum of others lies on the strong-field side and stays close

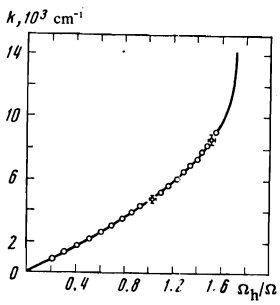

FIG. 6

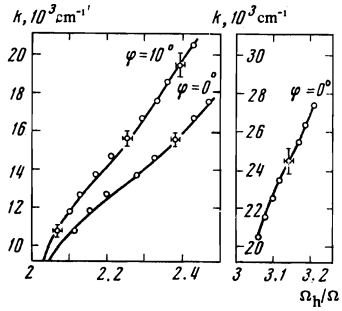

FIG. 7

FIG. 6. Comparison of calculated and experimental spectra in the region of the first hole resonance. Solid line—calculated spectrum. The points show the experimental data obtained with a sample 0.144 mm thick.

FIG. 7. Comparison of calculated and experimental spectra of cyclotron waves near the second and third hole resonances. $\varphi = 0$ at $\mathbf{H} \parallel C_1$, $\mathbf{H} \perp C_3$, d = 0.064 mm.

to resonance over its entire extent. The spectrum of the magnetosonic wave is very close to the long-wave CW spectrum in the region of the first hole resonance, so that when damping is taken into account the two spectra practically merge. An impression is therefore gained that it is not always possible to verify experimentally that the MSW continues beyond the first hole resonance. Figure 6 shows the calculated spectrum of the MSW and CW together with the experimental points obtained with a sample 0.064 mm thick. The error bars denote the absolute errors due to the inaccuracy with which the sample thickness, the magnetic field, and its orientation with respect to the axes were measured. We see that the theory agrees well with experiment.

The experimental plot of dR/dH (see Fig. 3) near the first CR line indicates the presence of oscillations of two types, with equal periods but with different amplitudes. In accordance with the theory, these oscillations are due to excitation in the plate of symmetrical and antisymmetrical fields, the former being more damped with increasing longitudinal component of the electric field on approaching the turning point of the spectrum. Each successive oscillation of one type corresponds to a change of unity in the integer number of waves spanned by the thickness of the plate. Only under this condition does the experimental dispersion curve agree with the theoretical ones, and its slope in the limit of the strong field corresponds to the data given in the literature (see[8]). The experimental spectra for all the CW were constructed in similar fashion.

In accordance with Fig. 1, in the magnetic field interval defined by $1 < \Omega_h/\Omega < 1.71$ there should exist also a short-wave CW with anomalous dispersion. However, as seen from Fig. 2, the oscillation amplitude corresponding to this CW is much smaller than for the long-wave CW. To observe this amplitude it is necessary to have much thinner samples (several microns), which would make it possible to reduce the influence of the oscillation background of the long-wave CW. In addition, the short-wave CW are apparently easier to excite and a resonator in which there is an electric-field component perpendicular to the surface of the sample.

A comparison of the experimental and theoretical CW spectra near the second and third CR harmonics is shown in Fig. 7. Here, too, there is good qualitative and quantitative agreement.

There is also agreement between the calculated and experimental amplitude characteristics of the oscillations due to the CW for different CR harmonics. Unfortunately, the oscillation amplitude for the first resonance line is not known exactly, owing to the already mentioned apparatus effects, but the ratio of the amplitudes of the second and third lines, which is equal to approximately six (cf. Fig. 5), is the same as obtained by calculation (cf. Fig. 2). The shape of the envelope of the oscillations also agrees with the predictions. For example, it is asymmetrical for the second harmonic and the damping is stronger on the side of the resonance line.

No short-wave CW with anomalous dispersion were observed for the higher CR harmonics, just as in the case of the first harmonic; this is due to the much smaller contribution they make to the impedance and to the worse excitation conditions, due to the smaller transverse electric-field component.

Rotation of the magnetic field in the trigonal plane changes the period and the amplitude of the oscillations. As the direction of **H** deviates from that of $\mathbf{C}_1$, the spectral lines become steeper and come closer to the resonant frequencies. Figure 7 shows the theoretical and experimental CW spectra for the second CR harmonic at an angle 10° between **H** and $\mathbf{C}_1$. At larger angles the calculation in the present paper no longer holds, since one of the electronic effective masses begins to increase strongly (as does also the radius of the orbit), and electronic CR begin to fall into the region of the hole CR.

This circumstance calls for an exact account of the spatial dispersion not only in the hole part of the conductivity but also in the electronic part. Experiment shows, on the other hand, that when $\mathbf{H} \parallel \mathbf{C}_2$, the magnetosonic wave (without allowance for its separation from the CW) no longer reaches the first hole CR, or in other words, the CW spectrum practically coincides with the resonance line. A detailed investigation of this question will be the subject of a separate article.

In conclusion, the authors thank A. A. Galkin for interest in the work and É. A. Kaner for a useful discussion.

[1] S. J. Buchsbaum and J. K. Golt, Phys. Fluids 4, 1514 (1971).

[2] É. A. Kaner and V. G. Skobov, Usp. Fiz. Nauk 89, 367 (1966) [Sov. Phys.-Uspekhi 9, 480 (1967)].

[3] M. S. Khaĭkin, L. A. Fal'kovskiĭ, V. S. Édel'man and R. T. Mina, Zh. Eksp. Teor. Fiz. 45, 1704 (1963) [Sov. Phys.-JETP 18, 1167 (1964)].

[4] J. Kirsch, Phys. Rev. 133, A1390 (1964).

[5] G. A. Williams, ibid. 139, A771, 1965.

[6] D. S. Mclachlan, ibid. 147, 368 (1966).

[7] V. S. Édel'man, Zh. Eksp. Teor. Fiz. 54, 1726 (1968) [Sov. Phys.-JETP 27, 927 (1968)].

[8] G. E. Smith and G. A. Williams, IBM J. Res. Dev. 8, 276 (1964).

[9] É. A. Kaner and V. G. Skobov, Fiz. Tverd. Tela 6, 1104 (1964) [Sov. Phys.-Solid State 6, 0000 (1964)].
[10] P. M. Platzman and W. M. Walsh, Phys. Rev. Lett. 15, 784 (1965).
[11] N. B. Brovtsyna and V. G. Skobov, Zh. Eksp. Teor. Fiz. 56, 694 (1969) [Sov. Phys.-JETP 29, 379 (1969)].
[12] V. S. Édel'man, ZhETF Pis. Red. 9, 302 (1969) [JETP Lett. 9, 177 (1969)].
[13] V. P. Naberezhnykh, D. É. Zherebchevskiĭ and V. L. Mel'nik, ibid. 13, 150 (1971) [13, 105 (1971)].
[14] J. Nakahara, H. Kawamura and Y. Sawada, Phys. Lett. A31, 271 (1970).
[15] J. Nakahara, H. Kawamura and Y. Sawada, Phys. Rev. 3, 3155 (1971).
[16] M. Ya. Azbel' and É. A. Kaner, Zh. Eksp. Teor. Fiz. 32, 896 (1957) [Sov. Phys.-JETP 5, 730 (1957)].
[17] V. S. Édel'man and M. S. Khaĭkin, ibid. 49, 107 (1965) [22, 77 (1966)].
[18] A. P. Korolyuk, ibid. 49, 1009 (1965) [22, 701 (1966)].
[19] F. G. Bass, A. Ya. Balnk and M. I. Kaganov, ibid. 45, 1081 (1963) [18, 747 (1964)].
[20] V. L. Mel'nik, Fizika kondensirovannogo sostoyaniya (Condensed State Physics), Trudy, Physico-technical Institute of Low Temperatures 11, 15 (1971).

Translated by J. G. Adashko
19